

# NUMERICAL MODELLING OF A MICROREACTOR FOR THERMOCATALYTIC DECOMPOSITION OF TOXIC COMPOUNDS

Paweł Józwik<sup>1</sup>, Michał Karcz<sup>2\*</sup>, Janusz Badur<sup>2</sup>

<sup>1</sup> Military University of Technology, ul. Kaliskiego 2, 00-908 Warszawa, Poland

<sup>2</sup> Polish Academy of Sciences, Institute of Fluid Flow Machinery, ul. Fiszerza 14, 80-231 Gdańsk, Poland

In this paper a three-dimensional model for determination of a microreactor's length is presented and discussed. The reaction of thermocatalytic decomposition has been implemented on the base of experimental data. Simplified Reynolds-Maxwell formula for the slip velocity boundary condition has been analysed and validated. The influence of the Knudsen diffusion on the microreactor's performance has also been verified. It was revealed that with a given operating conditions and a given geometry of the microreactor, there is no need for application of slip boundary conditions and the Knudsen diffusion in further analysis. It has also been shown that the microreactor's length could be practically estimated using standard models.

**Keywords:** microreactor, modelling, slip boundary conditions, CFD

## 1. INTRODUCTION

A reactor is usually considered to be a microreactor when its characteristic dimensions fall below one millimetre (Aoki et al., 2007; Chen et al., 2007). In the case of a microscale there is a considerable growth concerning the ratio of surface area to volume in comparison with standard reactors, such as gas turbine combustors (Badur, 2003). A simultaneous downscaling of channel dimensions and gas velocity lowering leads to a laminar flow with a very low  $Re$  number (Aoki et al., 2004). In general, laminar flow tends to block mass, momentum and energy transfer in the cross-flow direction, and the main mixing mechanism is governed by molecular diffusion. Small dimensions of microchannels and rarefactions of gases, as in the case of low pressure and high temperature, also make continual models with standard boundary conditions unsuitable for a numerical description of the process occurring at microscale (Karniadakis et al., 2005). As a result, an important issue arises in determining the possibility of using a particular model with slip/jump boundary conditions at the wall. It should be noted that the number of available measurements which can serve for model validation at the micro scale is relatively small. Particularly in relation to flows with chemical reactions there is no any publicly available comparative data which can be employed successfully for verification of boundary conditions that include velocity slip, temperature and concentration jump at the wall.

Catalytic surface reactions in the direct vicinity of walls coated with active layers are very often present in technical situations (Aoki et al., 2007; Duran et al., 2010). For thermal decomposition reactions these active layers are often built on the base of Ni alloys (Olafsen et al., 2006). For instance an Ni<sub>3</sub>Al-based

\*Corresponding author, e-mail: [michal.karcz@imp.gda.pl](mailto:michal.karcz@imp.gda.pl)

alloy is highly resistive to oxidation and has also sufficient strength at elevated temperatures (Józwiak et al., 2010). In this study, Ni<sub>3</sub>Al based microchannels have been numerically considered.

Computational fluid dynamics (CFD) allows to model heat and fluid flow processes in reactors of different types (Badur, 2003). Relevant issues concerning numerical modelling of combustion processes in microscale have already been presented in several papers (Chen et al., 2007; Norton and Vlachos, 2003; Xu and Yu, 2005). A model of catalytic combustion in a honeycomb set of microchannels has been described in a previous study by Deutschmann et al. (2000). A similar geometrical set has also been employed in the present consideration.

In this paper, results of different numerical analyses are presented. At first, a velocity slip model is validated using experimental data for a microchannel flow of argon. Next, the velocity slip model and the Knudsen diffusion model for the considered shape of microreactor is checked. In the last section, results of numerical analysis for decomposition of toxic compounds are shown. Instead of hazardous gases such as mustard gas and sarin, alternate hydrocarbon substances i.e. acetone and isooctane, that have a similar rate of thermocatalytic oxidation decomposition over the Ni<sub>3</sub>Al foil surface, have been employed. The main aim of the computations is to estimate the proper length of a microreactor sufficient to reduce the concentration of toxic compounds below an emergency level.

## 2. DESCRIPTION OF THE NUMERICAL MODEL

### 2.1. Model of fluid in bulk

The basic set of equations for computational fluid dynamics together with species transport equations can be written in the following manner, Badur (2003):

$$\frac{\partial}{\partial t} \begin{Bmatrix} \rho \\ \rho \vec{v} \\ \rho e \\ \rho Y_k \end{Bmatrix} + \text{div} \begin{Bmatrix} \rho \vec{v} \\ \rho \vec{v} \otimes \vec{v} \\ \rho e \vec{v} \\ \rho Y_k \vec{v} \end{Bmatrix} + \text{div} \begin{Bmatrix} 0 \\ p \vec{I} \\ p \vec{v} \\ 0 \end{Bmatrix} = \text{div} \begin{Bmatrix} 0 \\ \vec{\tau}_c \\ \vec{q}_c + \vec{\tau}_c \vec{v} \\ \vec{J}_k \end{Bmatrix} + \begin{Bmatrix} 0 \\ \rho \vec{S}_v \\ \rho S_e \\ \rho S_k \end{Bmatrix} \quad (1)$$

where  $\rho$  – mixture density,  $\vec{v}$  - velocity vector,  $Y_k$  – mass fraction of  $k$  mixture compound,  $e$  – total energy,  $p$  – static pressure,  $\vec{\tau}_c$  – total diffusive momentum flux,  $\vec{q}_c$  – total diffusive heat flux,  $\vec{J}_k$  - diffusive flux of  $k$  mixture compound,  $\vec{S}_v$  - momentum source,  $S_e$  - energy source and  $S_k$  – source of  $k$  mixture compound.

This set of equations is valid for all coordinate systems and possesses a universal form that allows to employ different constitutive relations. Every single physical process can be described within this framework via addition of new evolution equations (as for turbulence). Solutions can be determined using numerical methods for time and space discretization such as the finite volume method (FVM) or finite element method (FEM), which lead to the transformation of differential equations (1) into a set of nonlinear algebraic equations solved in an iterative manner. An important issue concerns the proper setting for conditions at boundaries of discretized geometrical domains. It is particularly important in the case of microchannels since some slip/jump effects may occur at the wall due to gas rarefaction.

### 2.2. Model of fluid in boundary layer

The mean free path of molecules for air at standard conditions is approximately equal to  $\lambda \approx 65 \text{ nm}$

(Karniadakis et al., 2005). When the characteristic length scale of the channel is comparable with the mean free path of molecules, the gas velocity at the wall is not zero, and the number of molecule collisions is insufficient to sustain a thermodynamic equilibrium (Xu and Yu, 2005). For a description of flow conditions, the Knudsen number is employed, which relates the mean free path to the characteristic channel dimension.

$$Kn = \frac{\lambda}{d} \quad (2)$$

It is assumed that for  $Kn < 0.001$  the standard model with zero velocity at the wall may be employed successfully. For  $Kn = (0.001 \div 0.1)$  the standard model can be employed only with an assumed velocity slip, temperature and concentration jump conditions at the walls (Xu and Yu, 2005; Duan and Muzychka, 2007; Jebauer and Czerwińska, 2007). There is also a transition region in the range of  $Kn = (0.1 \div 10)$ . It is assumed that for  $Kn > 10$  all continual models fail (Karniadakis et al., 2005). It is a result of gas rarefaction and compressibility effects (Morini et al., 2005).

In the case of constant temperature processes that occur in gases with  $Kn < 0.1$  only the velocity slip condition, that originally comes from Maxwell's findings (Maxwell, 1879), is of practical significance. Taking into account considerations of other contributors (Karniadakis et al., 2005; Xu and Yu, 2005), the velocity slip can be written in an extended Reynolds-Maxwell form as:

$$\vec{v}_{\text{slip}} = \left( \frac{2-f}{f} \right) \lambda \frac{1}{2} (\text{grad } \vec{v} + \text{grad}^T \vec{v}) \vec{n} + \frac{3}{4} \frac{\mu}{\rho T} (c_{vT} \text{grad } T + c_{vC} \text{grad } C_k) \quad (3)$$

where  $f$  – Maxwellian coefficient for momentum accommodation,  $\vec{n}$  – a wall normal vector,  $\mu$  – dynamic viscosity,  $\rho$  – density,  $T$  – temperature,  $C_k$  – the concentration of  $k$  compound of the mixture and  $c_{vT}$ ,  $c_{vC}$  are temperature and concentration mobility coefficients, respectively. The momentum accommodation coefficient depends on the type of fluid and wall material, and usually is selected from the range of  $0.7 < f < 1.0$  (Duan and Muzychka, 2007; Ewart et al., 2007).

### 2.3. Multicomponent diffusion model

In the case of a laminar mixture flow, where transport processes strongly depend on molecular diffusion, it is important to properly estimate mass, momentum and heat diffusion coefficients. There is a possibility to employ a single viscosity and thermal conductivity coefficient for the whole mixture. On the other hand, mass diffusion coefficients are treated separately for every compound in the mixture. For bulk flow, in the simplest form, diffusive flux,  $\vec{J}_k$ , is based on Fick's gradient hypothesis. In the case of a multicomponent mixture flowing through a microchannel, an effective diffusion coefficient should include molecular and Knudsen effects, by using a Bosanquet-type approximation (Yakabe et al., 2000; Mu et al., 2008):

$$\frac{1}{D_k^{\text{eff}}} = \frac{1}{D_k^{\text{mol}}} + \frac{1}{D_k^{\text{K}}} \quad (4)$$

The molecular diffusion coefficient is derived from a binary diffusion coefficient  $D_{kl}$  through the simplified formula (Yakabe et al., 2000):

$$D_k^{\text{mol}} = \frac{1 - X_k}{\sum_{l \neq k} \frac{X_l}{D_{kl}}} \quad (5)$$

These coefficients can be estimated from the Chapman-Enskog theory, or in the case of elevated temperatures, by using the Fuller method (Reid and Sherwood, 1966). The Knudsen diffusion

coefficient has the standard form (Mu et al., 2008):

$$D_k^K \approx 48.5d \sqrt{\frac{T}{M_k}} \quad (6)$$

where the microchannel characteristic dimension  $d$  is to be found.

#### 2.4. Model of catalytic reaction

Two cases are considered in the present study i.e. air/acetone mixture and air/isooctane mixture. It is assumed that there are no site species involved in surface reactions and thus only gas phase species are considered. It is also assumed that there is no coke formation during microreactor operations and products of thermocatalytic oxidation do not deposit on the catalyst surface.

Changes of species,  $k$ , concentration in the mixture due to chemical processes can be modelled via a volumetric source term,  $S_k$ , in the transport equation (1). As long as the considered reactions are catalytic, it was assumed that the source term  $S_k$  for a particular species can be formulated only in finite volumes adjacent to the microreactor wall. It is schematically presented in Fig. 1.

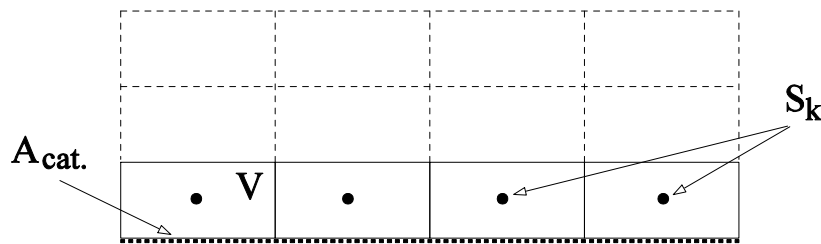


Fig. 1. Cross-section through the finite volumes in the wall vicinity where source terms  $S_k$  are formulated for every  $k$  compound of mixture

In general, the rate of species production/depletion depends on all relevant reactions ( $r$ ) occurring simultaneously, in which compound,  $k$ , takes part in (Badur, 2003):

$$S_k = M_k \sum_{(r)} \nu_{k(r)} R_{(r)} = M_k \sum_{(r)} \nu_{k(r)} \left\{ k_{(r)} \prod_k [X_k]^{v_{k(r)}} \right\} \quad (7)$$

The volumetric reaction rate,  $R_{(r)}$ , for non-reversible reaction ( $r$ ), is related to the forward rate constant,  $k_{(r)}$ , and reactant molar concentrations.

The final products for thermocatalytic oxidation of hydrocarbon based substances are mainly  $\text{CO}_2$  and  $\text{H}_2\text{O}$ . Since there is no detailed description of the decomposition mechanism over the  $\text{Ni}_3\text{Al}$  catalyst surface for a species under consideration, we decided to employ a simplified single-step non-reversible reaction in the form of:

- a) for air/acetone mixture:  $\text{C}_3\text{H}_6\text{O} + 4\text{O}_2 \rightarrow 3\text{H}_2\text{O} + 3\text{CO}_2$
- b) for air/isooctane mixture:  $\text{C}_8\text{H}_{18} + 12.5\text{O}_2 \rightarrow 9\text{H}_2\text{O} + 8\text{CO}_2$

Both reactions occur in a high excess of oxygen. Thus oxygen concentration is practically constant along the catalyst wall and the surface reaction rate can be simplified to the first order expression with respect to the acetone/isooctane concentration in the catalytic surface vicinity. The relevant rate constant,  $k_{\text{cat}}$ , of acetone/isooctane depletion, related to the unit of surface area, has been recalculated

from the experimental reaction rate presented in Table 1 under specified conditions (Jóźwik, 2010). The recalculation was performed under the following assumptions: -monolithic reactor; -Ni<sub>3</sub>Al foil thickness 50µm; -dimension of single catalytic specimen ca. 10<sup>-3</sup>×10<sup>-3</sup> m; -total mass of catalytic specimens 0.5×10<sup>-3</sup> kg; -density of Ni<sub>3</sub>Al foil 7509.3 kg/m<sup>3</sup>; -constant temperature of the process; -linear dependency of the reaction rate on mole concentration. During recalculation it was also assumed that the experimentally obtained rate constant (see Table 1) is an average value for mole fraction drop from 2000 ppm to 0 ppm. Thus after simple mathematical transformations, taking into account the main assumptions listed above, the rate constant  $k_{cat}$  values were estimated with unit [m<sup>3</sup>/(m<sup>2</sup><sub>cat</sub> s)].

Table 1. An experimental thermocatalytic oxidation rate of acetone/isooctane over Ni<sub>3</sub>Al foil estimated at GHSV= 40000h<sup>-1</sup> under the lowest possible temperature which is sufficient to obtain a full conversion from the initial mole fraction i.e. 2000 ppm (Jóźwik, 2010)

Species	Temperature [°C]	Experimental reaction rate [g/(g <sub>catalyst</sub> s)]
acetone	600	0.124
isooctane	700	0.151

To obtain the volumetric reaction rate,  $R_{(r)}$  (mol/m<sup>3</sup> s) consistent with the volumetric source term  $S_k$ , the surface reaction rate should be divided by the height of the computational cell adjacent to the microreactor wall ( $A_{cat}/V_{cell}$ ). Therefore, in the case of single surface reactions the source term (7) can be finally rewritten into the form:

$$S_k = M_k V_k k_{cat} [X_k] \left( \frac{A_{cat}}{V_{cell}} \right) \quad (8)$$

This model is valid for atmospheric pressure only under the assumption of a constant temperature in the microreactor for both considered cases (i.e.  $T=600^\circ\text{C}$  for air/acetone mixture and  $T=700^\circ\text{C}$  for air/isooctane mixture). It is also assumed that the unit surface based rate constant  $k_{cat}$  is independent of GHSV in the considered operational range of the microreactor.

### 3. MAIN ASSUMPTIONS FOR MODELLING

For the steady state flow analysis a CFD solver Fluent was employed. This finite volume based code allows one to solve the three-dimensional heat and fluid flow problems concerned with chemical reactions. It also allows for the addition of user defined subroutines programmed in C++ for problems that fall outside the capability of the standard version of code.

A single channel, located in the middle part of the considered microreactor has been chosen for further consideration. The geometry of the channels in the honeycomb set with characteristic dimensions are presented in Fig. 2.

The channel under consideration has been divided into some blocks that have been discretized by means of a structured numerical grid, steeply refined in the normal wall direction. Initial tests allowed to use the numerical grid to ensure that further refinement did not influence the computational results.

In the standard numerical practice, flow in channel with a characteristic dimension of approximately 10<sup>-3</sup> m is usually treated as a no-slip flow (Duan and Muzychka, 2007). As long as the main issue is the estimation of the minimal channel length and the reaction rate for slip flow is always higher than for no-slip flow (Xu and Yu, 2005), an assumption of zero velocity at the wall will lead to some overestimation of the channel length. Therefore, a possible numerical error connected with this

assumption should increase the safe margin of the reactor length. Despite this fact however, additional tests have been performed to assess the influence of gas velocity slip.

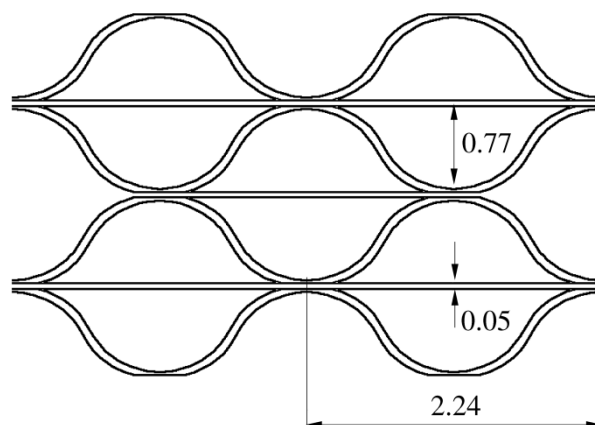


Fig. 2. The channels set cross-section (not in scale) – all dimensions are in [mm]

At the channel inlet, a uniform distribution of velocity, temperature and species mass fraction has been stated. Four values of gas velocity have been considered, namely 0.5; 1.0; 5.0 and 10.0 m/s (it roughly corresponds to volumetric flow rate of gas, 20; 40; 200 and 400 ml/min respectively). The maximum level of mole fraction for a toxic compound has been assumed at 25 ppm from the channel inlet. The minimum reactor length has been estimated under the assumption that it should be sufficient to reduce the toxic compound mole fraction to a safe level of around 0.15 ppm at the outlet.

In the microreactor, a laminar and incompressible flow has been assumed due to several factors: microscale dimensions of the channel, small gas velocity flowing through it and small pressure gradients. Chemical reactions are usually accompanied by changes in temperature of the reacting mixture. On the other hand, due to a small concentration of utilised species, the heat reaction input can be omitted. The microreactor scale additionally minimises the temperature nonuniformity (Xu and Yu, 2005). It has been also assumed that the reactor is ideally isolated to sustain the catalytic reaction, thus avoiding temperature drop along the channel and eliminating the need for thermal transpiration modelling (Badur, 2003). Therefore, the problem has been simplified to an isothermal one. It was also assumed that the active catalytic surface structure of the reactor can be treated as a homogeneous one and there is no deposition of any products on the catalyst surface during operation.

For closing the set of balance equations (1), it is necessary to formulate some closures that relate particular variables and allow to describe fluid properties. In the present case, an equation of state has been employed for the mixture of ideal gases under incompressibility condition in the form of:

$$\rho = \frac{P_{\text{ref}}}{RT \sum_k \frac{Y_k}{M_k}} \quad (9)$$

where  $k = \text{N}_2, \text{O}_2, \text{H}_2\text{O}, \text{CO}_2, \text{C}_3\text{H}_6\text{O}$  (acetone) or  $\text{C}_8\text{H}_{18}$  (isooctane).

The standard SIMPLE (semi-implicit method for pressure-linked equations) method has been used for pressure-velocity coupling. The second order upwind schemes have been employed for the solution of the convection term in transport equations. The diffusion terms have been central-differenced with the second order accuracy as well. The detailed methodology of numerical integration regarding the set of governing equations in the reacting mixture can be found in Badur (2003).

## 4. RESULTS OF NUMERICAL ANALYSIS

### 4.1. Influence of slip velocity conditions

Two numerical tests have been performed to assess the applicability of the slip velocity condition at the wall. At first, a validation of the numerical algorithm is presented. Two numerical models have been considered – one with a no-slip condition (zero velocity at the wall), and a second with a velocity slip according to a simplified Reynolds-Maxwell model (3), where only velocity gradient is taken into account. Numerical results have been compared with experimental data concerning microchannel flow of argon by Pitakarnnop (2009). A rectangular microchannel has been considered with the characteristic dimensions: height  $H = 1.84 \mu\text{m}$ , width  $W = 21.2 \mu\text{m}$  and length  $L = 5000 \mu\text{m}$ . The experiment concerns mass flow rate changes of flowing argon with different ratio between the inlet and outlet static pressure  $p_0/p_1$ , for a constant outlet pressure of 2 kPa and 50 kPa (Pitakarnnop, 2009). Results are presented in the subsequent diagrams in Fig. 3 and Fig. 4.

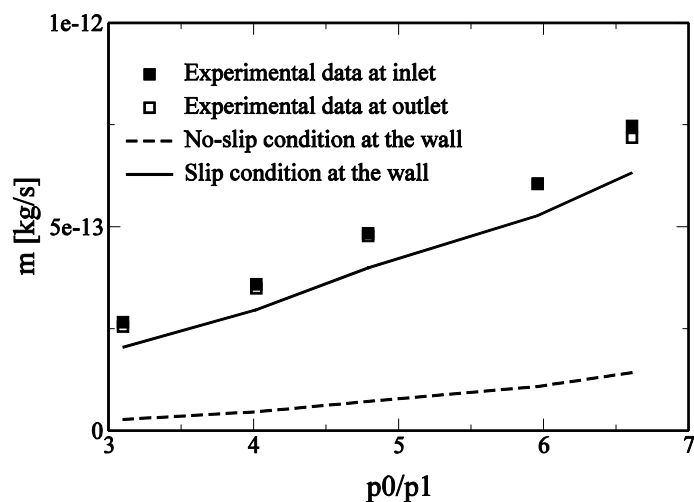


Fig. 3. Comparison between models with and without slip condition at the wall – outlet static pressure  $p_1 \approx 2\text{kPa}$  (experimental data from Pitakarnnop (2009))

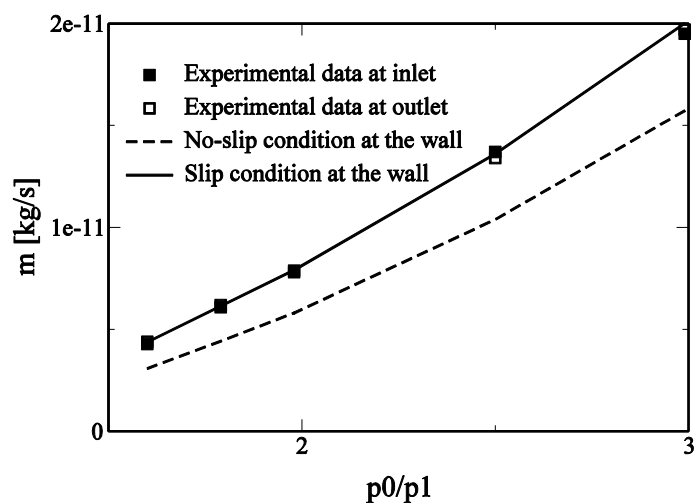


Fig. 4. Comparison between models with and without slip condition at the wall – outlet static pressure  $p_1 \approx 50\text{kPa}$  (experimental data from Pitakarnnop (2009))

In the case of the implemented slip velocity condition at the wall, the numerical results agree very well with the experimental data for moderate pressure close to atmospheric one (50 kPa) in Fig.4. For a more rarefied gas (2kPa), the slip condition leads to mass flow rate underestimation (of about 20%) under an assumed pressure drop in Fig. 3. However, this error is considerably lower than a no-slip condition, when the numerically obtained mass flow rate is even 80% lower than the experimental one. It should be reminded, that for strongly rarefied gases (with static pressure  $p \approx 2\text{kPa}$ , and corresponding to Knudsen number  $Kn \approx 1$ ), such a noticeable error can be easily linked to the questionable applicability of continual models in the transition region ( $Kn = 0.1 \div 10$ ), Karniadakis et al. (2005).

The second numerical test has concerned the microreactor channel under investigation, and has made it possible to assess the operational range for which the velocity slip condition is necessary to be employed. A single channel of the microreactor with the length  $L = 0.02\text{ m}$  has been considered. Tests have been conducted for air/acetone mixture under a range of pressure from 0.1 to 100kPa, which roughly corresponds to changes for the Knudsen number in the range of  $Kn = (0.005 \div 0.5)$ .

The influence of slip velocity conditions on the computed mass flow rate under the constant reactor pressure drop  $\Delta p = 5\text{ Pa}$  and constant process temperature of  $T = 600^\circ\text{C}$  has been investigated. Changes in the mass flow rate are estimated with the slip condition at the wall related to the mass flow rate with an imposed zero velocity condition at the wall are presented in the diagram (Fig.5).

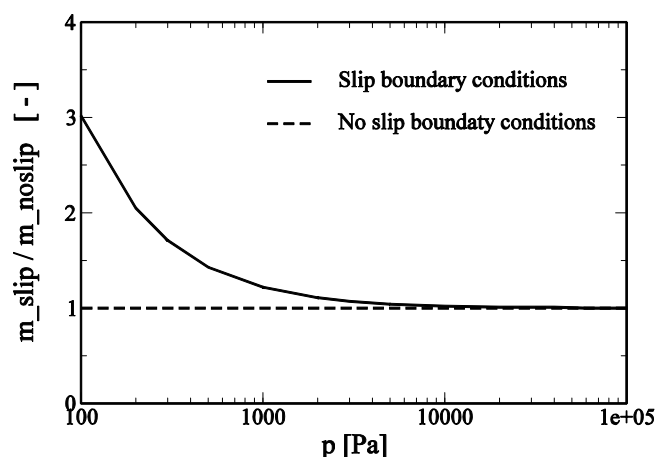


Fig. 5. Impact of velocity slip/noslip conditions at the wall on the computed mass flow rate in microchannel

It is clear that slip conditions become important only when the operating pressure is lower than 5 kPa. When atmospheric pressure is considered, as in a real situation, the performance of the investigated reactor can then be modelled without slip conditions at the wall.

#### 4.2. Influence of diffusion model

Several tests of the diffusion model described by Equations (4)–(6) have been performed for the air/acetone mixture under a pressure ranging between 0.1 to 100 kPa, assuming there was a constant pressure drop in the reactor  $\Delta p = 5\text{ Pa}$  and constant process temperature  $T = 600^\circ\text{C}$ . Additionally, an influence of the channel characteristic dimension  $d$  changes have been evaluated and presented in Fig. 6.

The influence of the term concerning Knudsen diffusion for the considered geometrical case (channel dimension  $\sim 10^{-3}\text{ m}$ ) and under atmospheric pressure is rather negligible. Its participation in the effective diffusion coefficient is lower than that of 0.01%. As a consequence Knudsen diffusion, described by Equation (6) can be virtually omitted during further modelling.



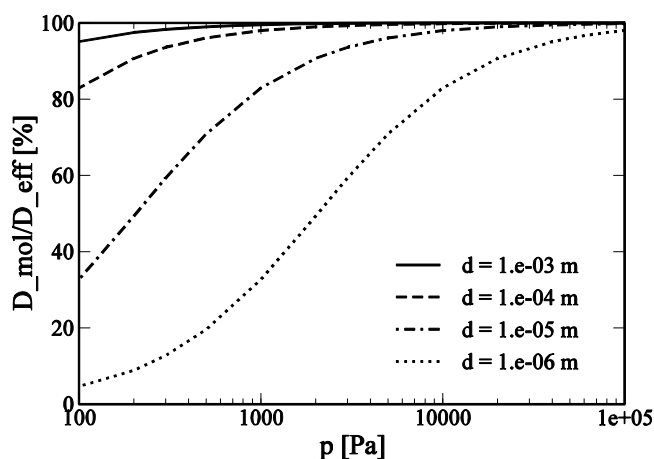


Fig. 6. Estimated influence of operating pressure and channel characteristic dimensions on the related molecular diffusion coefficient to an effective diffusion coefficient for air/acetone mixture

### 4.3. Estimation of the minimal reactor length

Longitudinal changes for the mole fraction of a toxic compound under thermocatalytic decomposition reaction along the investigated microchannel are presented in Fig. 7.

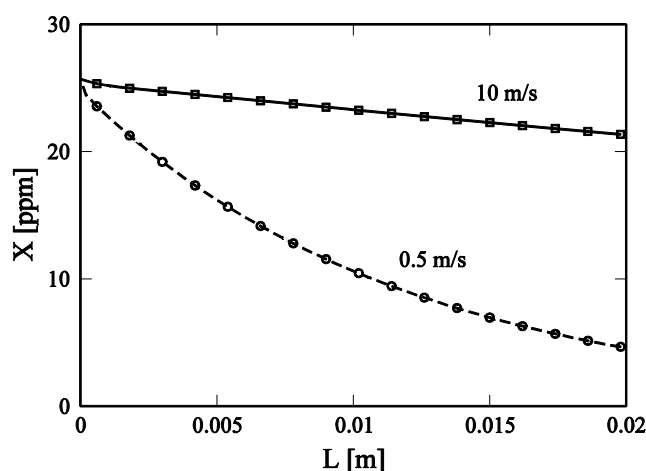


Fig. 7. Acetone mole fraction along the reactor channel wall ( $L_R = 0.02$  m) for two characteristic gas velocities – lines indicate results by standard model; symbols indicate results for model with slip velocity condition and Knudsen diffusion

It should be underlined that for all the presented cases there are practically no differences between the standard model with no-slip velocity condition at the wall and the model that includes Knudsen diffusion and slip velocity condition. The longitudinal changes of mole fraction reveal a dependency on gas velocity. There is a considerable drop in the acetone mole fraction for  $v = 0.5$  m/s, and rather a slow change for  $v = 10$  m/s. The laminar mode of flow limits mass transport towards the wall. In the case of lower volumetric flow rate, there is a sufficient time for every portion of contaminated air to be brought from the bulk to the catalytic surface by the molecular diffusion process. Thus the characteristic curve in Fig. 7 is steeper than the relevant curve for higher velocity. In the inlet section of the channel, where reactants concentrations are relatively high and where the still developing velocity profile promotes better mixing near the walls, there is also a more pronounced drop in the acetone mole fraction.

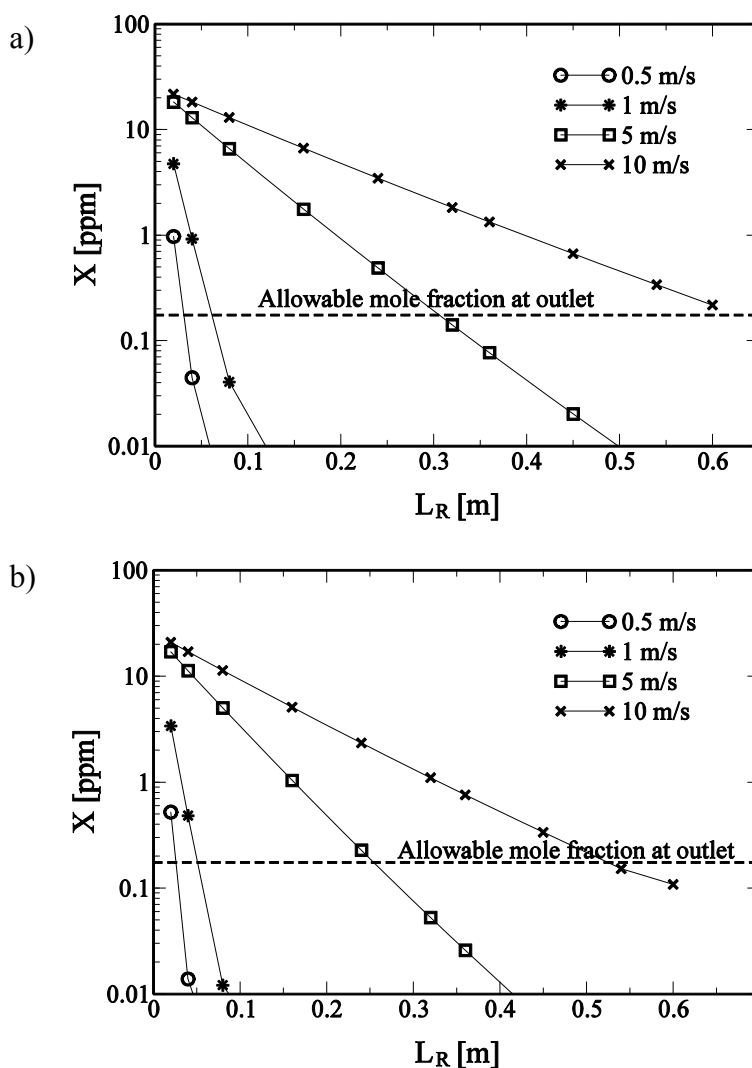


Fig. 8. Changes in outlet mass weighted average mole fraction for a different reactor length  $L_R$  in the function of velocity for contaminated air with regards to: a) acetone (for constant  $T = 600^\circ\text{C}$ ) and b) isooctane (for constant  $T = 700^\circ\text{C}$ ) respectively

In Fig. 8. acetone a) and isooctane b) recorded changes in the average outlet mole fraction. These changes are due to different channel lengths and gas velocities for both of the substances involved. Results show that an increasing velocity lowers the reactor effectiveness, as illustrated in Fig. 7. In order to fully neutralise toxic substances present in the air, a greater area of an active, catalytic surface is needed for higher velocity. In the case of isooctane, the reactor's length is somewhat shorter than that for acetone - due to a higher rate of reaction implemented on the basis of experimental data.

## 6. CONCLUSIONS

The original methodology of the three-dimensional numerical analysis for thermal catalytic microreactors used in treatment of contaminated air is presented in this paper. A successful validation of the implemented model with slip condition at the wall has been performed using experimental data of microchannel flow of argon that is to be found in the literature. A possible impact of imposing the velocity slip condition on the investigated microreactor performance is also estimated. It is now confirmed that for a given geometry and operational parameters (temperature and pressure), there is practically no necessity for modification of zero velocity conditions at the wall. A simultaneous analysis of mixture compounds diffusion modelling has indicated that Knudsen diffusion influences

results only for low pressure, and for very tight channels. The thermocatalytic decomposition reaction of toxic compounds has been modelled through employing some experimental data related to the active surface area. The data extrapolated via the implemented numerical model have made it possible to assess the minimal length of the microreactor channels, which provide a safe level of toxic compound concentration at the system outlet.

## SYMBOLS

$A$	surface area, $m^2$
$e$	total specific energy, J/kg
$C$	mole concentration, $mol/m^3$
$d$	mean dimension of channel, m
$f$	tangential momentum accommodation coefficient
$GHSV$	gas hourly space velocity, 1/h
$H$	channel height, m
$\vec{I}$	Gibbs' idemfactor
$\vec{j}$	diffusion flux of mixture component, $kg/(s\ m^2)$
$k_{cat}$	thermocatalytic decomposition rate constant, $m^3/(m^2_{cat}\ s)$
$k_{(r)}$	forward rate constant for volumetric reaction ( $r$ ), 1/s
$L$	channel length, m
$L_R$	total length of the reactor, m
$M$	molecular weight, kg/kmol
$p$	pressure, Pa
$\vec{q}$	total diffusive heat flux, $W/m^2$
$R_{(r)}$	volumetric reaction rate, $mol/(m^3\ s)$
$R$	gas constant, $J/(mol\ K)$
$T$	temperature, K
$\vec{v}$	velocity vector, m/s
$V$	volume, $m^3$
$W$	channel width, m
$X$	mole fraction
$[X]$	molar concentration, $mol/m^3$
$Y$	mass fraction
<i>Greek symbols</i>	
$\varepsilon$	energy dissipation rate, $m^2/s^3$
$\lambda$	mean free path, m
$\nu$	stoichiometric coefficient
$\mu$	dynamic viscosity, $kg/(m\ s)$
$\rho$	mixture density, $kg/m^3$
$\vec{\tau}$	total diffusive momentum flux, Pa
$\dot{\omega}$	rate of the mixture compound production/destruction, $mol/(m^3\ s)$
<i>Superscripts</i>	
$eff$	effective
$K$	Knudsen
$mol$	molecular

*Subscripts*

<i>cat</i>	catalytic
<i>cell</i>	computational cell
<i>k, l</i>	components of mixture
<i>(r)</i>	reaction number
<i>R</i>	reactor
<i>ref</i>	referential
<i>slip</i>	slip

## REFERENCES

- Aoki N., Hasebe S., Mae K., 2004. Mixing in microreactors: effectiveness of lamination segments as a form of feed on product distribution for multiple reactions. *Chem. Eng. J.*, 101, 323-331. DOI: 10.1016/j.cej.2003.10.015
- Aoki N., Yube K., Mae K., 2007. Fluid segment configuration for improving product yield and selectivity of catalytic surface reactions in microreactors. *Chem. Eng. J.*, 133, 105-111. DOI: 10.1016/j.cej.2007.02.006.
- Badur J., 2003, *Numerical modelling of sustainable combustion In gas turbines*. IFFM Publishers, Gdańsk. (in Polish)
- Chen G.-B, Chen C.-P., Wu C.-Y., Chao Y.-C., 2007. Effects of catalytic walls on hydrogen/air combustion inside a micro-tube. *Appl. Catal. A*, 332, 89-97. DOI:10.1016/j.apcata.2007.08.011
- Deutschmann O., Maier L.I., Riedel U., Stroemman A.H., Dibble R.W., 2000. Hydrogen assisted catalytic combustion of methane on platinum. *Catal. Today*, 59, 141-150. DOI: 10.1016/S0920-5861(00)00279-0.
- Duan Z., Muzychka Y.S., 2007. Slip flow in non-circular microchannels. *Microfluid Nanofluid*, 3, 473-484. DOI: 10.1007/s10404-006-0141-4.
- Duran J.E., Mohseni M., Taghipour F., 2010. Modeling of annular reactors with surface reaction using computational fluid dynamics (CFD), *Chem. Eng. Sci.*, 65, 1201-1211. DOI: 10.1016/j.ces.2009.09.075.
- Ewart T., Perrier P., Graur I., Méolans J.G., 2007. Tangential momentum accommodation in microtube, *Microfluid Nanofluid*, 3, 689-695. DOI: 10.1007/s10404-007-0158-3.
- Jebauer S., Czerwińska J., 2007. Implementation of velocity slip and temperature jump boundary conditions for microfluidic devices. *ITFR Reports*, 5, 1-50.
- Józwik P., 2010. *Final report of research project OR00004905 on: Military application of micro, ultra and nanocrystalline alloys Ni<sub>3</sub>Al - Technology demonstrator of thermoactive elements for contaminated air treatment systems*, Military University of Warsaw (in Polish)
- Józwik P., Bojar Z., Winiarek P., 2010. Catalytic activity of Ni<sub>3</sub>Al foils in decomposition of selected chemical compounds. *Inżynieria Materialowa*, 3, 654-657.
- Karniadakis G., Beskok A., Aluru N., 2005. Microflows and Nanoflows - Fundamentals and Simulation. In: Antman S.S., Marsden J.E., Sirovich L. (Eds.), *Interdisciplinary Applied Mathematics*, 29, Springer.
- Maxwell J.C., 1879. On stresses in rarified gases arising from inequalities of temperature. *Phil. Trans. R. Soc. London*, 170, 231-256.
- Morini G.L., Lorenzini M., Spiga M., 2005. A criterion for experimental validation of slip-models for incompressible rarefied gases through microchannels. *Microfluid Nanofluid*, 1, 190-196. DOI: 10.1007/s10404-004-0028-1.
- Mu D., Liu Z.-S., Huang C., Djilali N., 2008. Determination of the effective diffusion coefficient in porous media including Knudsen effects, *Microfluid Nanofluid*, 4, 257-260. DOI: 10.1007/s10404-007-0182-3.
- Norton D.G., Vlachos D.G., 2003. Combustion characteristics and flame stability at the microscale: a CFD study of premixed methane/air mixtures. *Chem. Eng. Sci.*, 58, 4871-4882. DOI: 10.1016/j.ces.2002.12.005.
- Olafsen A., Daniel C., Schuurman Y., Raberg L.B., Olsbye U., Mirodatos C., 2006. Light alkanes CO<sub>2</sub> reforming to synthesis gas over Ni based catalysts. *Catal. Today*, 115, 179-185. DOI: 10.1016/j.cattod.2006.02.053.
- Pitakarnnop J., Varoutis S., Valougeorgis D., Geoffroy S., Baldas L., Colin S., 2010. A novel experimental setup for gas microflows, *Microfluid Nanofluid*, 8, 57-72. DOI: 10.1007/s10404-009-0447-0
- Reid R.C., Sherwood T.K., 1966. *The properties of gases and liquids*, McGraw-Hill Book Company, New York.

- Xu B., Ju Y., 2005. Concentration slip and its impact on heterogeneous combustion in a micro scale chemical reactor. *Chem. Eng. Sci.*, 60, 3561-3572. DOI: 10.1016/j.ces.2005.01.022.
- Yakabe H., Hishinuma M., Uratani M., Matsuzaki Y., Yasuda I., 2000. Evaluation and modeling of performance of anode-supported solid oxide fuel cell, *J. Power Sources*, 86, 423-431. DOI: 10.1016/S0378-7753(99)00444-9.